

# An optimization-based model discrimination framework for selecting an appropriate reaction kinetic model structure during early phase pharmaceutical process development

Maitraye Sen, Alonso J. Arguelles, Stephen D. Stamatis, Salvador García-Muñoz, Stanley Kolis  
Synthetic Molecule Design and Development, Lilly Research Laboratories, Eli Lilly & Company, 1400 West  
Raymond Street, Indianapolis, Indiana 46221, United States

## Supplemental material

(Cited references are present in the bibliography of the main manuscript)

### S1. Calculating the sensitivity matrix

The dimensions of the sensitivity matrix  $S$  given in the equation<sup>18</sup> below are  $N \times P$ , where  $N$  is the total number of data points and  $P$  is the number of parameters.

$$S_{ij} = \frac{\partial g_{dn}}{\partial \theta} = \begin{bmatrix} \frac{\partial g_{11}}{\partial \theta_1} | u_1 & \cdots & \frac{\partial g_{11}}{\partial \theta_p} | u_1 \\ \vdots & \ddots & \vdots \\ \frac{\partial g_{1n}}{\partial \theta_1} | u_1 & \cdots & \frac{\partial g_{1n}}{\partial \theta_p} | u_1 \\ \frac{\partial g_{21}}{\partial \theta_1} | u_1 & \cdots & \frac{\partial g_{21}}{\partial \theta_p} | u_1 \\ \vdots & \ddots & \vdots \\ \frac{\partial g_{dn}}{\partial \theta_1} | u_1 & \cdots & \frac{\partial g_{dn}}{\partial \theta_p} | u_1 \\ \frac{\partial g_{11}}{\partial \theta_1} | u_2 & \cdots & \frac{\partial g_{11}}{\partial \theta_p} | u_2 \\ \vdots & \ddots & \vdots \\ \frac{\partial g_{dn}}{\partial \theta_1} | u_2 & \cdots & \frac{\partial g_{dn}}{\partial \theta_p} | u_2 \\ \vdots & \ddots & \vdots \\ \frac{\partial g_{dn}}{\partial \theta_1} | u_r & \cdots & \frac{\partial g_{dn}}{\partial \theta_p} | u_r \end{bmatrix}$$

Here  $g_{dn}$  corresponds to the measurement of the  $d^{\text{th}}$  response variable at  $n^{\text{th}}$  time point,  $u_r$  is the experimental setting (or experimental condition) of the  $r^{\text{th}}$  experiment and  $\theta_p$  is the  $p^{\text{th}}$  parameter.  $N = DnTr$ , where  $D$  is the total number of response variables that can be

measured,  $n_T$  is the total number of time points at which a response variable is measured, and  $r$  is the different dynamic experimental runs. Each element of the sensitivity matrix corresponds to the partial derivative of a response variable with respect to a model parameter evaluated at a specific experimental condition. The layout of the matrix is such that a given row contains information about a specific time point, and that a given column contains information about a given parameter.

In this work, the sensitivity matrix was calculated numerically using a central finite difference expression for each partial derivative. A +10% and -10% perturbation was given to each parameter (one at a time). The ratio of the change in the response variables (due to the perturbation) to the total change in the parameter (20% in this case) was calculated. The range of perturbation was arbitrarily selected to approximate the Jacobian matrix. The Jacobian may change depending on the range and the initial parameter values selected. However, since Arrhenius expressions are exponential functions, the concavity is not expected to change. Even though the values of the matrix element will differ depending on the range and initial parameter values, the rank order of the parameters is not expected to change drastically. However, this is an approximation of the Jacobian and the user may need to run a brute-force analysis to arrive at an appropriate range and parameter values. To ensure dimensional consistency, a scaled sensitivity matrix ( $Z$ ) was used for the calculations as given in equation<sup>16</sup> below.

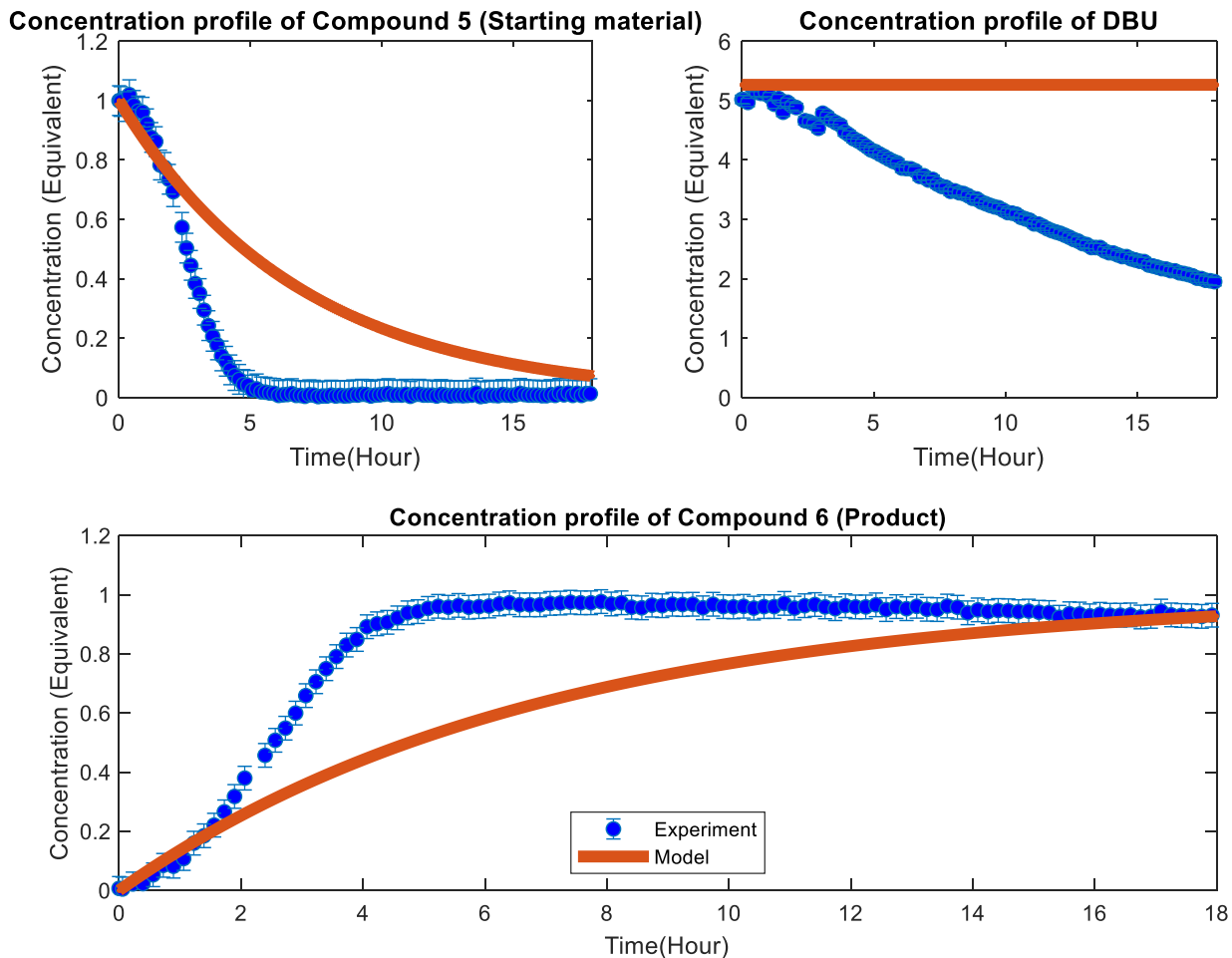
$$Z_{ij} = S_{ij} \frac{s_{\theta_j 0}}{s_{y_i}}$$

The elements of the sensitivity matrix were multiplied by a ratio of the uncertainty in parameter initial guesses ( $s_{\theta_j 0}$ ) and the variability in the experimental measurement ( $s_{y_i}$ ). The uncertainty in the initial guess of the parameter was quantified by assuming that the possible parameter values are normally distributed with a standard deviation of  $1/6^{\text{th}}$  of the parameter value.

## **S2. Fit of the kinetic model obtained from Mechanism a**

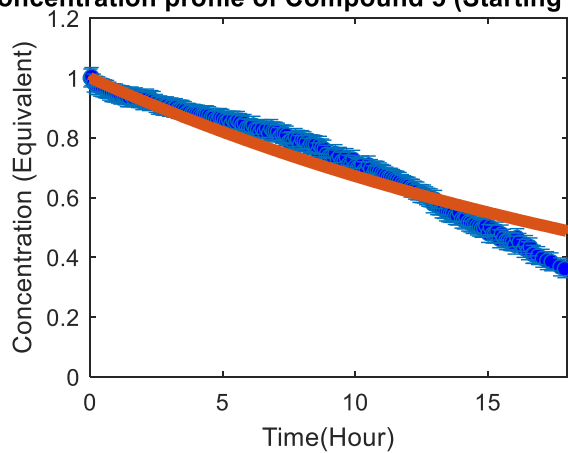
Figure A1 below presents the model validation of scheme a (Figure 3 in the main manuscript). The preliminary experiments reported in table 1 were used to parameterize the model. However, since

this mechanism assumes DBU as catalytic, it couldn't fit the concentration profile of DBU obtained from the experiments. Therefore, this kinetic model was rejected.

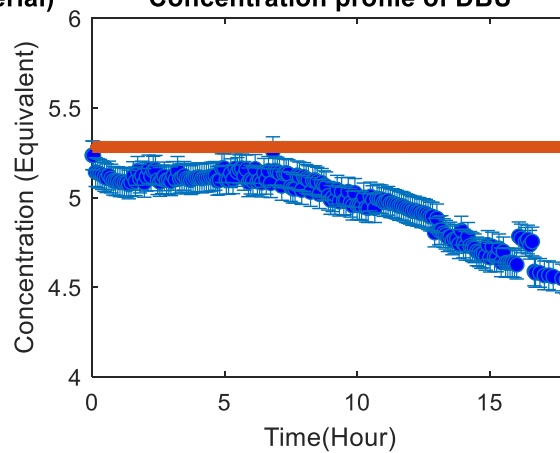


(a) Model fit of Experiment 1

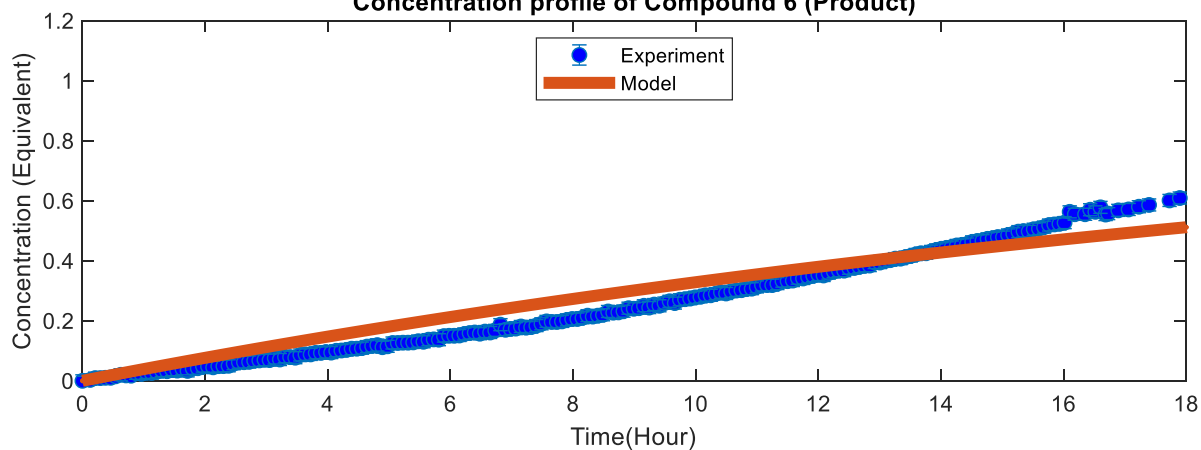
**Concentration profile of Compound 5 (Starting material)**



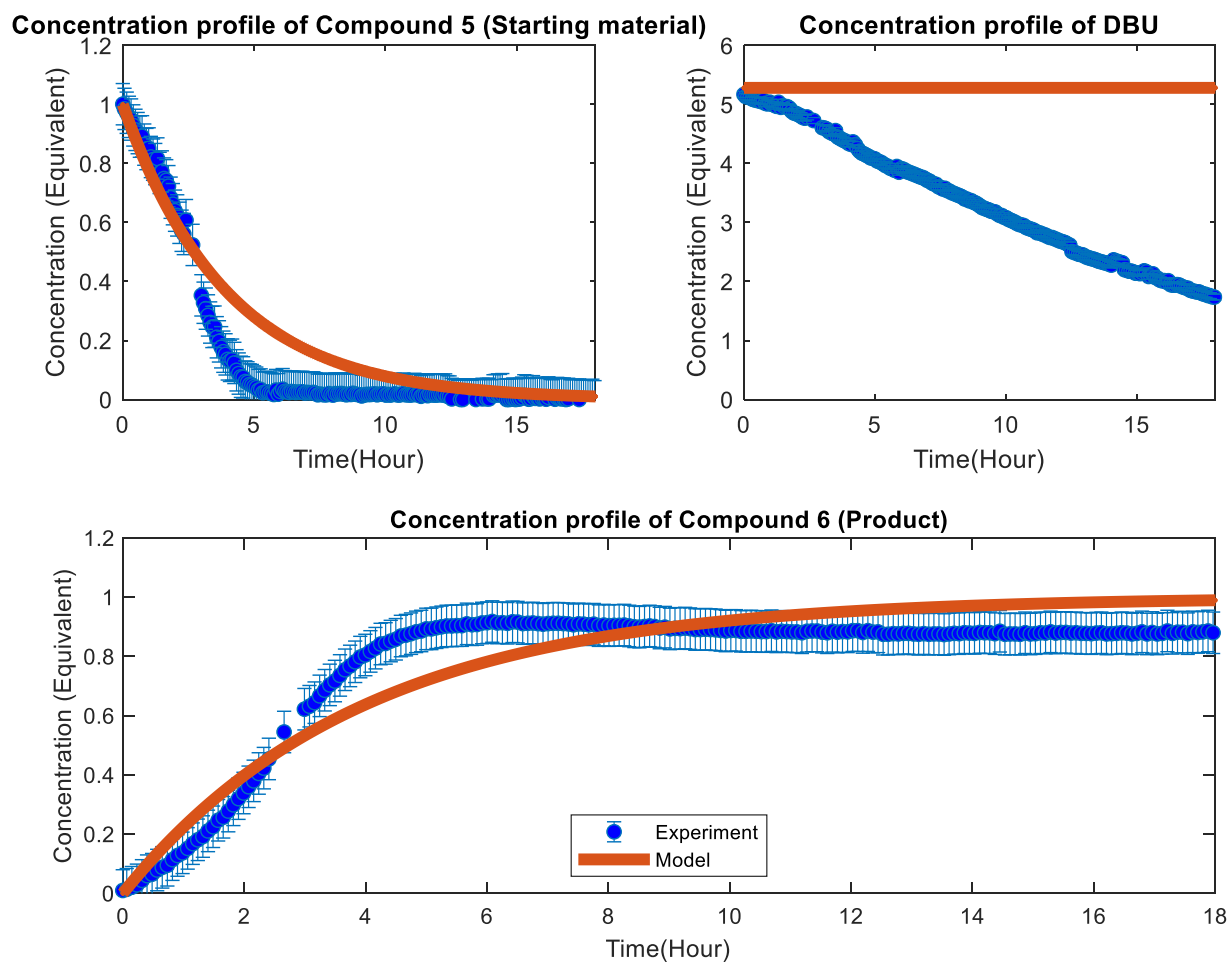
**Concentration profile of DBU**



**Concentration profile of Compound 6 (Product)**



**(b) Model fit of Experiment 2**



(c) Model fit of Experiment 3

**Figure A1: Fit of the preliminary experiments by the kinetic model developed from mechanism scheme a**

**S3. Model 1 parameter estimates (preliminary parameter estimation with estimability analysis)**

Table A1 below presents the parameter estimates of model 1 obtained from the preliminary experiments after incorporating estimability analysis.

<b>Model Parameter</b>	<b>Final Value</b>	<b>Initial Guess</b>	<b>Search Lower Bound</b>	<b>Search Upper Bound</b>
<b><math>A_1</math> (Fixed)</b>	$5.050 \times 10^{13}$	$5.050 \times 10^{13}$	$5.050 \times 10^{13}$	$5.050 \times 10^{13}$
<b><math>A_{.1}</math> (Fixed)</b>	$4.510 \times 10^9$	$4.510 \times 10^9$	$4.510 \times 10^9$	$4.510 \times 10^9$
<b><math>A_2</math> (Fixed)</b>	$1.263 \times 10^9$	$1.263 \times 10^9$	$1.263 \times 10^9$	$1.263 \times 10^9$
<b><math>A_{.2}</math> (Fixed)</b>	$3.189 \times 10^9$	$3.189 \times 10^9$	$3.189 \times 10^9$	$3.189 \times 10^9$
<b><math>A_3</math> (Fixed)</b>	$5.634 \times 10^6$	$5.634 \times 10^6$	$5.634 \times 10^6$	$5.634 \times 10^6$
<b><math>A_4</math> (Fixed)</b>	$4.880 \times 10^{11}$	$4.880 \times 10^{11}$	$4.880 \times 10^{11}$	$4.880 \times 10^{11}$
<b><math>E_1</math></b>	$39.315 \times 10^3$	$90 \times 10^3$	$1 \times 10^3$	$500 \times 10^3$
<b><math>E_{.1}</math></b>	$2.464 \times 10^3$	$71.146 \times 10^3$	$1 \times 10^3$	$500 \times 10^3$
<b><math>E_2</math></b>	$98.254 \times 10^3$	$96.28 \times 10^3$	$1 \times 10^3$	$500 \times 10^3$
<b><math>E_{.2}</math></b>	$101.006 \times 10^3$	$90 \times 10^3$	$1 \times 10^3$	$1000 \times 10^3$
<b><math>E_3</math></b>	$52.442 \times 10^3$	$48.21 \times 10^3$	$1 \times 10^3$	$500 \times 10^3$
<b><math>E_4</math></b>	$95.033 \times 10^3$	$75.634 \times 10^3$	$1 \times 10^3$	$500 \times 10^3$

**Table A1: Parameter values for Model 1 (post-estimability)**

**S4. Model 2 parameter estimates (preliminary parameter estimation with estimability analysis)**

Table A2 below presents the parameter estimates of model 2 obtained from the preliminary experiments after incorporating estimability analysis.

<b>Model Parameter</b>	<b>Final Value</b>	<b>Initial Guess</b>	<b>Search Lower Bound</b>	<b>Search Upper Bound</b>
$A_1$	$79.867 \times 10^5$	$138.606 \times 10^5$	$1 \times 10^5$	$200 \times 10^5$
$A_2$	$1 \times 10^{12}$	$0.398 \times 10^{12}$	$1 \times 10^5$	$1 \times 10^{12}$
$A_2$ <b>(Fixed)</b>	$4.674 \times 10^5$	$4.674 \times 10^5$	$4.674 \times 10^5$	$4.674 \times 10^5$
$A_3$	$36.111 \times 10^3$	$2.478 \times 10^3$	$1 \times 10^3$	$100 \times 10^3$
$A_4$ <b>(Fixed)</b>	$3.019 \times 10^7$	$3.019 \times 10^7$	$3.019 \times 10^7$	$3.019 \times 10^7$
$E_1$	$0.084 \times 10^6$	$0.085 \times 10^6$	$0.01 \times 10^6$	$1 \times 10^6$
$E_2$	$0.098 \times 10^6$	$0.0879 \times 10^6$	$0.01 \times 10^6$	$1 \times 10^6$
$E_{-2}$	$0.049 \times 10^6$	$0.070 \times 10^6$	$0.01 \times 10^6$	$0.9 \times 10^6$
$E_3$	$0.047 \times 10^6$	$0.050 \times 10^6$	$0.01 \times 10^6$	$1 \times 10^6$
$E_4$	$1 \times 10^6$	$0.087 \times 10^6$	$0.085 \times 10^6$	$1 \times 10^6$

**Table A2: Parameter values for Model 2 (post-estimability)**

**S5. Model 1 parameter estimates (adding MD-DOE in the data pool)**

Table A3 below presents the parameter estimates of model 1 obtained after adding the MD-DOE in the data pool.

<b>Model Parameter</b>	<b>Final Value</b>	<b>Initial Guess</b>	<b>Search Lower Bound</b>	<b>Search Upper Bound</b>	<b>Standard Error</b>
$A_1$ <b>(Fixed)</b>	$5.050 \times 10^{13}$	$5.050 \times 10^{13}$	$5.050 \times 10^{13}$	$5.050 \times 10^{13}$	
$A_{.1}$ <b>(Fixed)</b>	$4.510 \times 10^9$	$4.510 \times 10^9$	$4.510 \times 10^9$	$4.510 \times 10^9$	
$A_2$ <b>(Fixed)</b>	$1.263 \times 10^9$	$1.263 \times 10^9$	$1.263 \times 10^9$	$1.263 \times 10^9$	
$A_{.2}$ <b>(Fixed)</b>	$3.189 \times 10^9$	$3.189 \times 10^9$	$3.189 \times 10^9$	$3.189 \times 10^9$	
$A_3$ <b>(Fixed)</b>	$5.634 \times 10^6$	$5.634 \times 10^6$	$5.634 \times 10^6$	$5.634 \times 10^6$	
$A_4$ <b>(Fixed)</b>	$4.880 \times 10^{11}$	$4.880 \times 10^{11}$	$4.880 \times 10^{11}$	$4.880 \times 10^{11}$	
$E_1$	$111.361 \times 10^3$	$90 \times 10^3$	$1 \times 10^3$	$500 \times 10^3$	$1.246 \times 10^3$
$E_{.1}$	$75.188 \times 10^3$	$71.146 \times 10^3$	$1 \times 10^3$	$500 \times 10^3$	$1.901 \times 10^3$
$E_2$	$99.538 \times 10^3$	$96.280 \times 10^3$	$1 \times 10^3$	$500 \times 10^3$	$0.047 \times 10^3$
$E_{.2}$	$96.204 \times 10^3$	$90 \times 10^3$	$1 \times 10^3$	$10000 \times 10^3$	$0.093 \times 10^3$
$E_3$	$38.547 \times 10^3$	$48.210 \times 10^3$	$1 \times 10^3$	$500 \times 10^3$	$1.227 \times 10^3$
$E_4$	$93.469 \times 10^3$	$75.634 \times 10^3$	$1 \times 10^3$	$500 \times 10^3$	$1.459 \times 10^3$

**Table A3: Final parameter values for model 1**

## S6. Process contour generated from Model 2

Figure A2 below presents the process map where the product yield has been mapped as a function of the reaction temperature and molar equivalent of the starting material (compound 5) calculated with respect to a basis. The product yield is the % yield of the product (compound 6) with respect to a byproduct. The “red” region has the lowest product yield compared to the byproduct, and the “green” region has the highest product yield. This map was then used to identify a suitable process operating space.

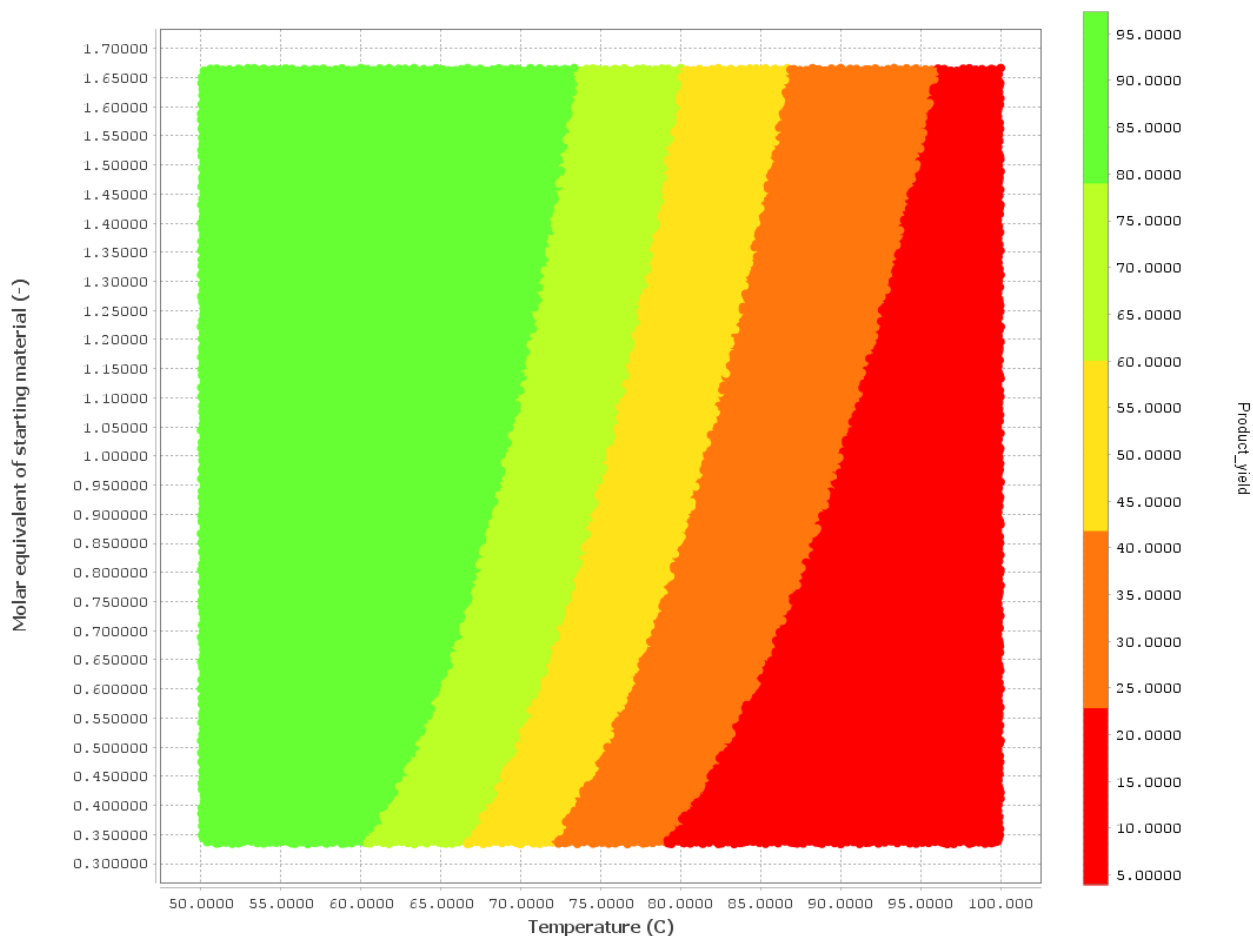


**Figure A2: Process Contour presenting the product yield as a function of temperature and molar equivalent of starting material charged**